Weight-bearing CT Technology in Musculoskeletal Pathologies of the Lower Limbs: Techniques, Initial Applications, and Preliminary Combinations with Gait-Analysis Measurements at the Istituto Ortopedico Rizzoli

Alberto Leardini, D.Phil[1] Stefano Durante, BSc[2] Claudio Belvedere, PhD[1] Paolo Caravaggi, PhD[1] Claudio Carrara, MEng[1] Lisa Berti, MD, Prof[1] Giada Lullini, MD[1] Claudia Giacomozzi, PhD[3] Gilda Durastanti, MEng[1] Maurizio Ortolani, BCA[1] Giuseppe Guglielmi, MD[4] Alberto Bazzocchi, MD, PhD[5]

[1] Movement Analysis Laboratory, IRCCS Istituto Ortopedico Rizzoli, Bologna, Italy
[2] Nursing, Technical and Rehabilitation Assistance Service, IRCCS Istituto Ortopedico Rizzoli, Bologna, Italy
[3] Department of Cardiovascular and Endocrine-Metabolic Diseases and Aging, Istituto Superiore di Sanità, Roma, Italy
[4] Department of Radiology, University of Foggia, Foggia, Italy
[5] Diagnostic and Interventional Radiology, IRCCS Istituto Ortopedico Rizzoli, Bologna, Italy

Address for correspondence Alberto Leardini, D.Phil, Movement Analysis Laboratory, IRCCS Istituto Ortopedico Rizzoli, Via di Barbiano 1/10, Bologna, 40136, Italy (e-mail: leardini@ior.it).

Semin Musculoskelet Radiol 2019;23:643–656.

Abstract

Musculoskeletal radiology has been mostly limited by the option between imaging under load but in two dimensions (i.e., radiographs) and three-dimensional (3D) scans but in unloaded conditions (i.e., computed tomography [CT] and magnetic resonance imaging in a supine position). Cone-beam technology is now also a way to image the extremities with 3D and weight-bearing CT. This article discusses the initial experience over a few studies in progress at an orthopaedic center. The custom design of total ankle replacements, the patellofemoral alignment after medial ligament reconstruction, the overall architecture of the foot bones in the diabetic foot, and the radiographic assessment of the rearfoot after subtalar fusion for correction of severe flat foot have all taken advantage of the 3D and weight-bearing feature of relevant CT scans. To further support these novel assessments, techniques have been developed to obtain 3D models of the bones from the scans and to merge these with state-of-the-art gait analyses.

Keywords
- cone-beam CT
- weight-bearing
- three-dimensional bone models
- gait analysis
- plantar pressure

Conventional medical imaging is a fundamental support for diagnosis of the musculoskeletal apparatus and for the assessment of pharmacologic, physical, surgical, prosthetic, and orthotic treatments. In addition, it is used during surgical interventions in orthopaedics for direct visual access to anatomical structures and implants. Medical imaging analysis has also been essential to develop new techniques and treatments. Radiography, computed tomography (CT), magnetic resonance imaging (MRI), and videofluoroscopy have been used massively in orthopaedics. A quick search in June 2019 (with search term "medical imaging orthopaedics") showed > 32,000 articles and nearly 2,700 reviews. Among these, only eight use cone-beam computed tomography (CBCT) technology, a recent fundamental development initially exploited only in oral and maxillofacial treatments.[1,2]

CBCT is an emerging medical imaging technique with the original feature of divergent radiographs (i.e., forming a cone), in contrast with the spiral slicing of conventional

Issue Theme Weight-bearing Musculoskeletal Imaging; Guest Editors, James F. Griffith, MB BCh, MRCP, FRCR, MD, FHKCR, FHKAM (Radiology) and Giuseppe Guglielmi, MD

DOI https://doi.org/10.1055/s-0039-1697939.
ISSN 1089-7860.

CT.[3,4] In the presence of a gantry, and with a radiographic source and a detection system opposed to the source, a large rotation of this system around the stationary patient on which the collimated beam is projected generates a complete volumetric three-dimensional (3D) data set. CBCT has become increasingly important in treatment planning and diagnosis initially for small anatomical areas, particularly in implant dentistry and interventional radiology.

Diagnosis and treatment of the musculoskeletal system possibly both needs static and dynamic measures for quantitative assessments. Human motion analysis, which usually implies kinematic, electromyographic, and plantar pressure measures, has been frequently conducted to identify anomalies in patterns of biomechanical variables, before and after interventions, in particular during the execution of activities of daily living, as well as during surgery. In contrast, static representations of anatomical structures are provided successfully using standard medical imaging. From CT and MRI devices, this can be obtained effectively in 3D, but the positions normally used (i.e., typically supine) are very far from those required of standard motor tasks.

In other words, with traditional devices it is very difficult to get medical imaging scans under realistic loading conditions for the lower limbs. Dynamic MRI can now provide image sequences of soft tissues during basic motor tasks, but the quality is rather poor, and 3D reconstructions are challenging. Roentgen-stereophotogrammetry can track small metal beads and metal devices from two radiographs also under loading conditions, but the process is demanding and applies only to metal implants of known 3D geometry. The same limitations apply to 3D videofluoroscopy, where 3D motion of a replaced joint, also during the execution of simple motor tasks, is estimated by videofluoroscopy and uses the computer-aided drafting model of the relevant prosthesis components. In general, either bidimensional (2D) pictures under load or 3D reconstructions in unloading conditions are accessible.

Medical imaging devices based on CBCT technology have recently entered the CT market for upper and lower limbs, that is, the extremities. These devices can now provide 3D images in loading conditions (weight-bearing computed tomography [WBCT]). This fundamental new feature offers relatively low radiation, high spatial resolution, and convenient ergonomy,[5–10] and as such it may have a promising role in making more precise diagnoses and assessments in various applications in orthopaedics and musculoskeletal disorders. In particular, the foot, ankle, and knee, but also the hand, wrist, and elbow, can finally benefit from this equipment because weight-bearing situations are fundamental to comprehend the functional mechanisms of these anatomical structures. The load can also be modulated and measured with the addition of easy-to-use devices, from full single- or double-leg upright postures to other similar postural conditions, with the leg and the joints under determined rotations and forces. This technique can definitely overcome traditional measures from planar radiographs that have long been used for geometric characterization of the overall architecture of the bones of the foot.[11]

In the present article, we analyze this recent technological development by reporting and discussing initial applications in our orthopaedic center.

Current Techniques and Applications at the Orthopaedic Center

CBCT scans were collected in several selected patients (OnSight 3D Extremity System, Carestream, Rochester, NY), either at the foot and ankle or at the knee, mostly in the single-leg upright posture. In a few minutes, the 3D rendering of the scan is made available automatically (example images of all these procedures can be found for the foot and ankle in ►**Fig. 1**). Virtual slicing of the 3D data set, along any preferred axis, can be performed to obtain CT Digital Imaging and Communications in Medicine (DICOM) images at a minimum distance of 0.26 mm. This data set is processed in Amira (Zuse Institute Berlin, FEI Visualization Sciences Group), with semiautomatic segmentation of each single bone, and it results in corresponding 3D models in STL format. The ground can also be segmented and used in 3D as a reference for the orientation of the transverse anatomical plane of the foot. The STL files are imported in MATLAB (MathWorks Inc., Natick, MA), in the technical reference frame of the CBCT device, thus with no anatomical meaning. An anatomical reference frame for the foot can be defined, for example with the vertical axis orthogonal to the ground plane and the anteroposterior axis along the most plantar points of the calcaneus and second metatarsal head. The mediolateral axis is the cross product of these two axes; all foot bones are realigned in this frame.

On these bone models, anatomical axes can be defined, according to traditional or novel techniques. An example is reported here for the calcaneus (►**Fig. 2**). Principal component analysis (PCA)[12–14] is able to calculate automatically the orthogonal axes of maximum, intermediate, and minimum variance of a cloud of points. If these are the surfaces of the calcaneus, because of the general anatomical conformation of the bone, this provides the longitudinal, vertical, and mediolateral axial directions, respectively (►**Fig. 2a**). The axes joining the most plantar or most dorsal anatomical landmarks of the bone can also be defined as other possible longitudinal directions, still in 3D (►**Fig. 2b**), more in keeping with the radiographic angle, such as the calcaneal inclination angle (CIA)[11,15,16] or calcaneal pitch angle.[17,18] For each of these axes, the inclination angle with respect to the ground can also be calculated in 3D, that is, in the plane orthogonal to the ground and containing the axis. Something very similar can be applied to any bone. In addition to this absolute inclination of a single bone, the relative orientation between two bones can be measured by calculating the 3D angle in between them. For the calcaneus and first metatarsus, for example (►**Fig. 2c**), the angle between their longitudinal axes is calculated, as already reported in the literature ("calcaneal-first metatarsal" [C1MA or CA-MT1][19,20] and the Hibb angle[18,21]).

Ankle Replacement

Total ankle replacement was developed as a long-term solution[22] to restore mobility as well as to alleviate pain in arthritic

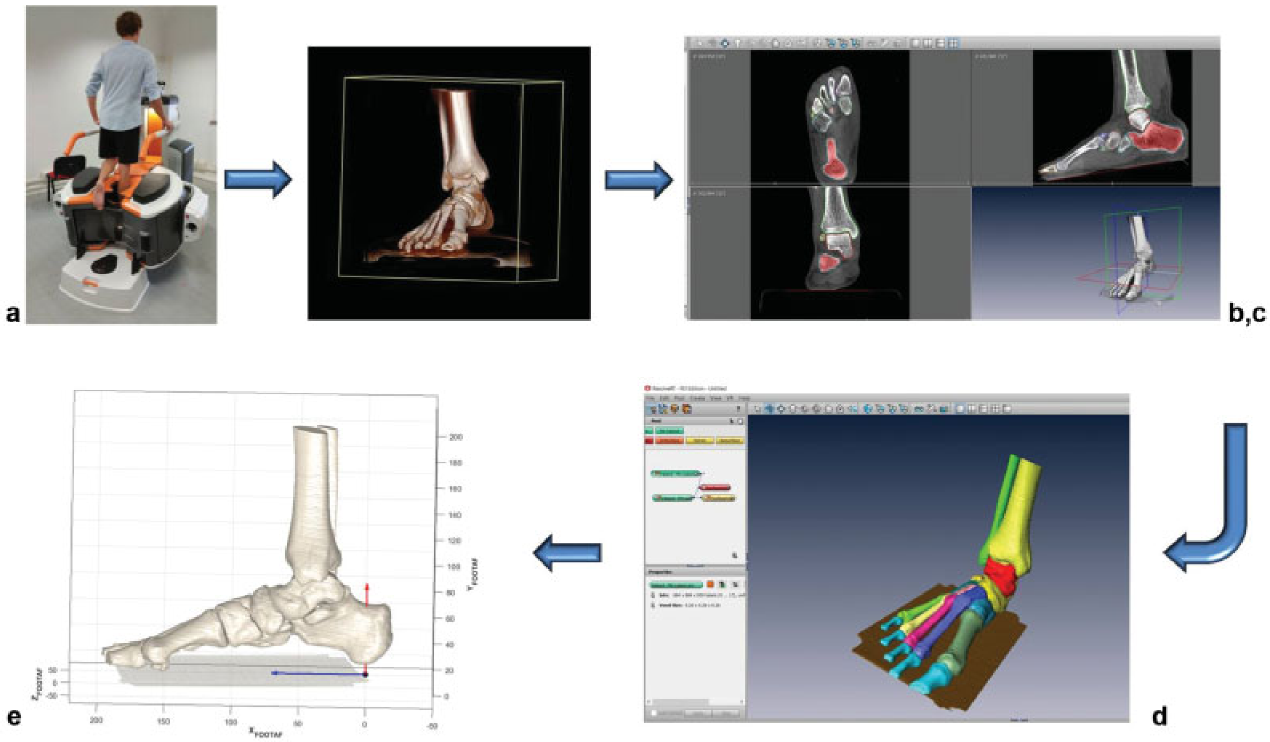

Fig. 1 The full process from weight-bearing computed tomography (WBCT) scans to three-dimensional (3D) bone models of the entire foot, from a normal subject (22-year-old man; height:179 cm; weight: 65 kg). (**a**) The subject in single-leg weight-bearing position during the cone-beam computed tomography scan. (**b**) The 3D volume rendering is available on an interactive screen a few minutes after the scan. (**c**) Process of foot bone segmentation (Amira software): identification of the silhouette of the calcaneus in the three anatomical planes and the 3D reconstruction of the entire foot. (**d**) All foot and ankle bone segments modeled separately (different colors); the ground segment is also depicted (in gray), still in the CBCT technical reference frame. (**e**) The same 3D model of the entire foot in STL format, once imported in MATLAB, after reorientation in the foot anatomical reference frame, in a nearly lateral view.

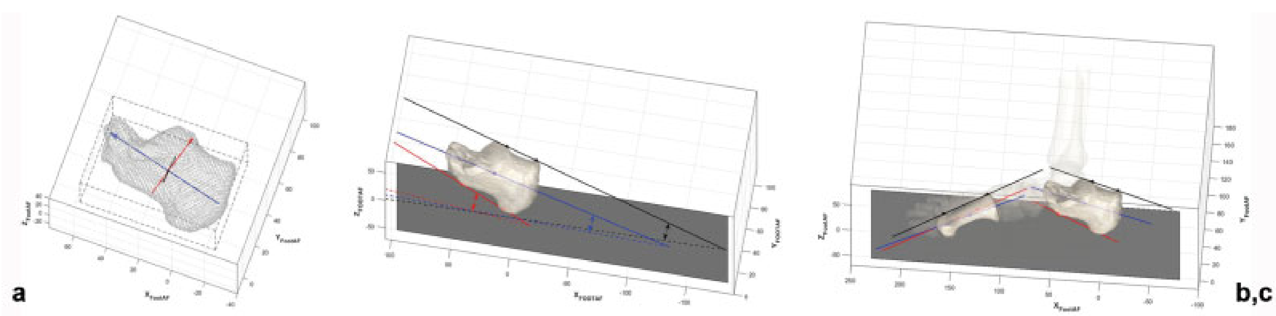

Fig. 2 Screenshots from the geometric analysis in MATLAB: the construction of various representations of the longitudinal axis of the calcaneus. (**a**) The original full bone model with the three axes from the principal component analysis (PCA) and the origin of the coordinate system at the centroid of the bone model. (**b**) Calculation of the absolute inclination angles for the calcaneus: for the PCA-based longitudinal axis (in blue) and for the other two techniques based, more traditionally, on most plantar (red) or most dorsal (black) anatomical landmarks. (**c**) Three-dimensional calculation of the relative angles between two bones: from the three representations of the longitudinal axis of the calcaneus (b) and three of the first metatarsus.

ankles,[22–25] with stability also easily achieved by arthrodesis. Moderately good clinical results were reported; however, size mismatch remains an important contributing factor to secondary complications,[22] particularly because the small numbers of indications have meant only a very small number of prosthesis designs and component sizes are available. Prosthesis customization has therefore the potential to improve clinical results by attuning designs to patient-specific dimensions. This is possible now by the technology called additive manufacturing, or 3D printing, where powders of the exact same traditional metals used in orthopaedic implants for decades are fused layer by layer to produce a compact 3D object.[26,27] Initial studies show that comprehensive procedures including medical imaging, joint modeling, prosthesis design, and 3D printing can be performed successfully to obtain custom-made ankle replacements, even applying innovative biomechanical designs.[28]

In an initial experience in our institution, an original established design of total ankle replacement is applied for the overall customization procedure. The BOX Ankle design, developed by some authors years ago,[23,29] is used here for this overall customization procedure. This takes advantage of WBCT, thanks to which joint alignments of the arthritic ankle and after-replacement alignment scenarios can be assessed in weight-bearing. The condition of the tibial mortise and syndesmosis, the tibiotalar and subtalar joint positions in the frontal and transverse planes, and the overall alignments are much better revealed. The scope of this preliminary study is to assess feasibility, quality, and effectiveness of prosthesis component customization to minimize size mismatch and improve outcomes prospectively. In this initial phase of the investigation and industrial production, standard instrumentation and original meniscal inserts are maintained, and several possible clinical cases are analyzed.

WBCT scan of the arthritic ankle is obtained in the single-leg upright posture, with axial alignment of the lower limb and pelvis (►**Fig. 3**). Patient-specific bone models are then obtained by semiautomatic segmentation. The standard prosthesis components are parameterized using Creo software (PTC, Boston, MA). Starting from a best fit standard size, corresponding custom prosthesis components are designed according to the best possible match of the bone models and alignment of the replaced joint. An optimized proximodistal level of the implant is searched for according to the quality and geometry of the bone. This customization therefore implies virtual, that is, in-silico, implantation of the components into the bone models, using Geomagic Control X software (3D Systems, Rock Hill, SC). Virtual bone resections corresponding to the custom-designed components are then performed using polygon manipulation. A comparative analysis between the standard and custom in-silico implantations is usually conducted using distance mapping and calculations of bone-to-prosthesis contact and resection volumes. Distance mapping (►**Fig. 3** shows a typical example) demonstrates the improved contact with the resected bone including better placement on the edge of the estimated cortical bone rim. The prosthesis-to-bone surface coverage increases on average by 6 to 10%.

Even outside this procedure of customization for the implants, the use of 3D modeling from WBCT can definitely improve prosthesis component size choice and its implantation and therefore support presurgical planning. This experience, although still limited to a few cases, demonstrates that ankle replacement customization can minimize mismatch through improved sizing and placement on bone. It indicates the value of further investigation, including clinical cases,

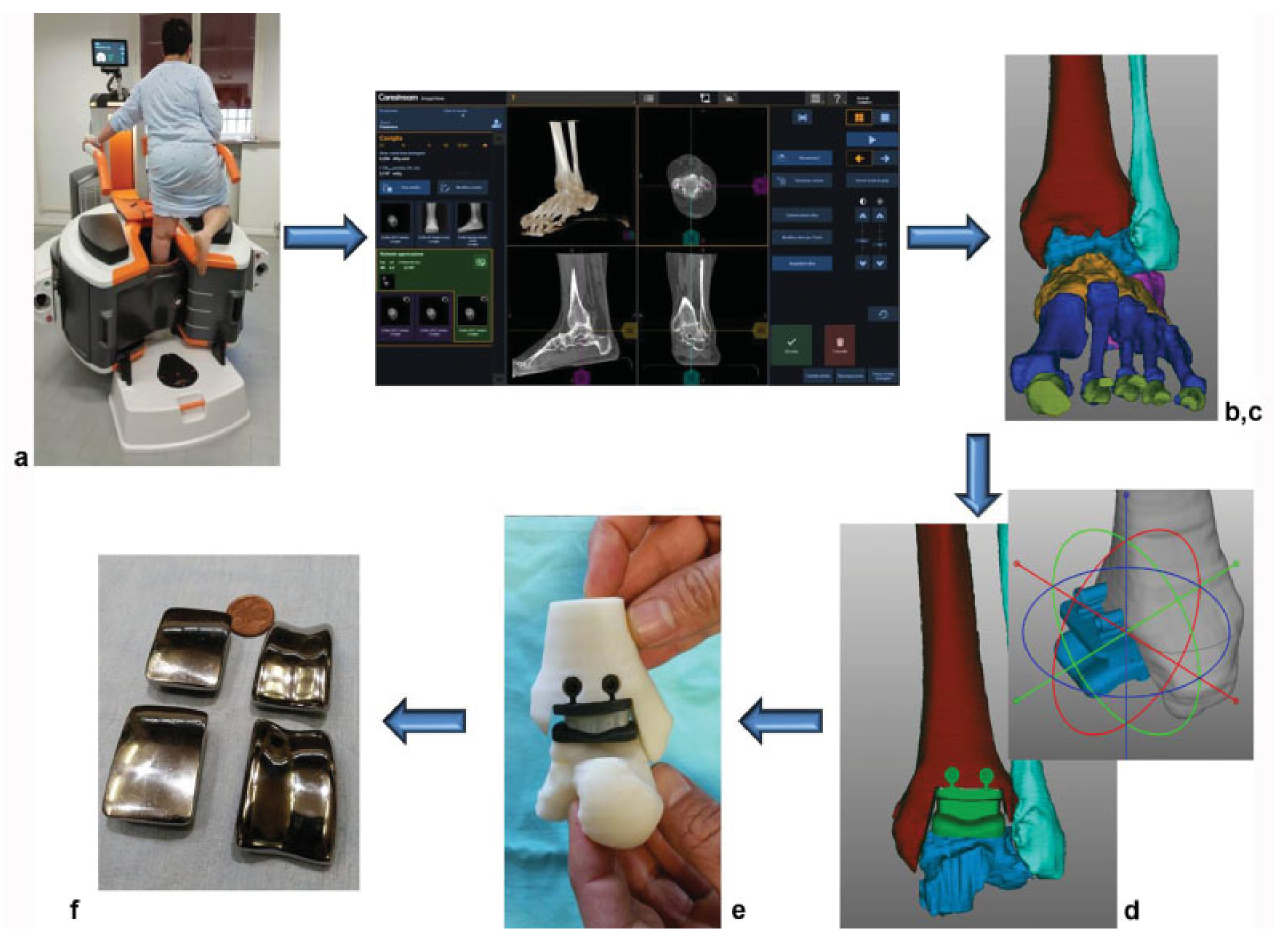

Fig. 3 The phases for design and manufacturing of personalized total ankle replacements. (**a**) The patient in the cone-beam computed tomography (CBCT) device for the scan. (**b**) Screenshot of the CBCT screen of the foot and ankle after the scan. (**c**) Arthritic ankle after three-dimensional (3D) bone model reconstruction. (**d**) Custom design: tailoring of the dimensions, virtual implantation, and bone preparation. (**e**) The final model of the replaced ankle is first 3D printed with cheap polymers for final check. (**f**) Eventually the final metal prosthesis components are obtained from additive manufacturing in cobalt chromium molybdenum powders and careful polishing.

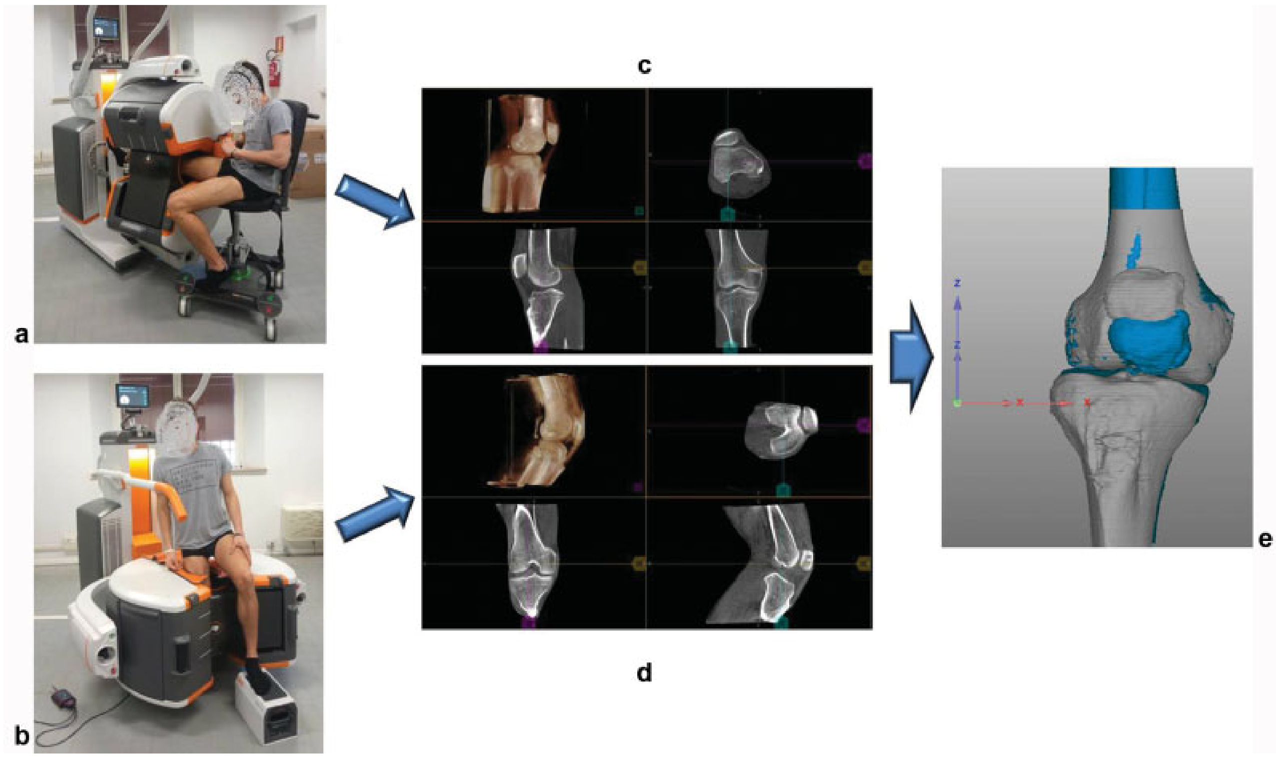

Fig. 4 Two scans from cone-beam computed tomography (CBCT) of a typical patient of the medial patellofemoral ligament study, (**a**) without weight-bearing and (**b**) with weight-bearing. In the latter, small connections for the simultaneous plantar pressure measurements during scanning can be depicted. Corresponding screenshots from the CBCT device, with the three anatomical plus the three-dimensional views (**c** and **d**, respectively). (**e**) Superimposition of the two corresponding knee joint reconstructions (blue and gray, respectively) after merging in space of the two proximal tibia bone models. The effect of weight and muscle actions on the patella's position is very considerable.

particularly the effects of customization on biomechanics, bone-to-prosthesis stress, and wear. The use of WBCT definitely enhances the potential of these procedures because of the realistic condition of the joint alignments, with limited radiation doses. It was also demonstrated that CBCT devices, in combination with state-of-the-art MRI,[30] can produce complete bone-plus-cartilage joint models. In the same article it was shown, however, that geometric design parameters are very sensitive to the quality of the medical images and to the algorithms for their analyses.

The present investigation on customization of ankle replacement is still limited by the narrow scope because of the present industrial constraints regarding instrumentation and inserts, as mentioned earlier. But in the near future, patient-specific instrumentation and custom polyethylene inserts will be introduced as well, for a full customization of the intervention. Only a few ankle specimens and a few patients have been analyzed so far. In the future, morphological analyses can certainly also be enhanced by motion measurements of the contralateral joint that would add a kinematic target to the design, to determine the appropriate position of the joint rotation axis, for example. Of course, with the same 3D model of the arthritic joint, other prosthesis designs could also be investigated.

Medial Patellofemoral Ligament Reconstruction at the Knee

Patellar instability is generally evaluated by conventional CT, in which the usual patient position is supine, with extended knee and relaxed muscles. However, it is well known from the literature that knee flexion along with quadriceps contraction, as representative of real knee joint-loading conditions, influences patellar motion significantly. Accordingly, these must be replicated when evaluating patellar instability via medical imaging. With this in mind, an investigational study was designed to compare the evaluation outcomes of patellar instability derived from using the standard assessment approach (supine by regular CT) with those derived from WBCT in patients treated surgically with medial patellofemoral ligament reconstruction for patellar instability at 5-year follow-up, after full functional recovery (►**Fig. 4**).

The analysis of several parameters typically adopted to describe patellar alignment, (i.e., patellar congruence and tilt angle) and tibial tuberosity-trochlear groove (TT-TG) distance was performed. Preliminary clinical data showed no instability or relapse of dislocation. As for imaging-based data derived from a regular CT in a supine position, the congruence and tilt angle were, on average, 13.0 ± 10.7 degrees and 7.3 ± 2.9 degrees, respectively, whereas the TT-TG distance was 11.5 ± 1.5 mm. Corresponding values in weight-bearing conditions by the same CBCT device were 16.1 ± 6.7 degrees, 9.3 ± 3.8 degrees, and 7.0 ± 2.5 mm, respectively. These preliminary values from a small sample of patients show remarkable differences between the two evaluation methods. In the presence of knee loading, in particular, the congruence and tilt angle are larger than in supine, whereas the contrary occurs for the TT-TG distance.

Diabetic Foot Biomechanics

The foot skeleton is a very complex structure and may change over the progression of several pathologies including the critical diabetic foot. In particular, the pathomechanics of diabetic foot ulceration were largely investigated with plantar loading measurements and also via human motion analysis.[31] Only rarely has medical imaging been used to investigate associated morphological alterations related to this pathology, mainly because of its static condition. Major limitations are that even though radiographs can be performed in weight-bearing conditions, they only offer 2D information, and even though CT scans offer 3D information they are normally performed in non–weight-bearing conditions. Of course bone alignments change considerably from non–weight-bearing to weight-bearing,[32] and only the latter offers a realistic representation of this structure during activities of daily living. These modern WBCT devices now allow 3D geometric measurements of the foot under load, finally giving access to the full bone architecture in weight-bearing, which is of particular value for diabetic foot assessments. In a preliminary study, diabetic feet in type 1 diabetes patients were analyzed using a CBCT device, in stationary weight-bearing, for bone and joint alignments to be assessed in 3D. Dynamic plantar loading was also collected, and possible correlations between these two measures were investigated. The study aimed at correlating dynamic plantar pressure measurements with the corresponding 3D bone alignments from WBCT.

DICOM files of both feet were obtained from WBCT scans in 20 diabetic foot patients. A series of 6 feet from the most compromised patients (4 male, type 1, 4 with neuropathy; 58 ± 16 years, 26 ± 2 kg/cm^2, 32 ± 11 years of disease [YOD], arch index 0.25 ± 0.02) was segmented, producing 3D models of all the 30 bones for each foot. MATLAB software was used (see earlier and ►**Figs. 1** and **2**) to perform automatic geometric calculations based on either anatomical landmarks and axes, or on PCA (►**Fig. 5**). Planar angles in all three anatomical plane projections and in 3D were calculated. In this preliminary analysis, metatarsal (M1–M5) and phalangeal (P1–P5) bones were analyzed, for their height from the ground (H_), together with absolute (A_) and relative (R_) orientations (i.e., phalanx-to-metatarsal, in the sagittal plane only). Pressure patterns were acquired (EMED q-100, Novel GmbH, Germany), registered and averaged over five consistent gait trials for each patient and foot.[33] For the selected feet (mean contact time: 0.68 ± 0.06 s), peak pressure (PP) and the pressure-time integral (PTI) were extracted at the hallux and at the first (M1), central, and fifth (M5) metatarsal bones. Pearson's correlation analysis (R v.3.4.3; The R Foundation) was conducted on all these parameters.

The following relevant ($R^2 > 0.6$) and statistically significant ($p < 0.05$) correlations were found. Increasing age, body mass index, and YOD strongly correlated with increasing dorsiflexion of lateral phalanxes (A_P4, A_P5, R_M4P4, and R_M5P5; $R^2 = 0.81$–0.94); YOD also correlated with central metatarsals' loss of height (maximum between H_M2, H_M3, and H_M4; $R^2 = 0.65$). Plantar loading increase at M1, either PP or PTI, positively strongly correlated with age ($R^2 = 0.88$) and with the same 3D parameters ($R^2 = 0.68$–0.84) and also with M1 loss of height (H_M1; $R^2 = 0.78$) and M2 elevation (H_M2; $R^2 = 0.71$). Central metatarsal loading increased with P5 plantarflexion (A_P5; $R^2 = 0.65$). PP and PTI strongly correlated with each other at every area.

The present measurements for plantar loading and bone architecture of the foot can be performed in similar conditions. Their combination has great potential and may provide fundamental new insights for a thorough assessment of diabetic foot complications. A relevant software tool has been developed and applied on diabetic feet, showing interesting, although very preliminary, correlations between these measurements. If confirmed over the whole sample of patients and feet, this will ideally help to design and assess more effective orthotic or surgical interventions.

Subtalar Fusion for Flat-Foot Surgical Correction

Acquired adult flatfoot is a very frequent deformity including valgus of the hindfoot, flattening of the medial longitudinal arch, and abduction of the forefoot. This is considered a complex 3D syndrome combining multiple static and dynamic deformities with pronation of the subtalar joint, which explains the difficulty of evaluation and hence of the indication for treatment. A comprehensive study is in progress, aimed at evaluating flatfoot deformities carefully and multi-instrumentally, with a combination of 3D static and dynamic parameters, respectively, from WBCT and functional gait analysis, both before and after surgery (Grice's technique). The subtalar joint and the rest of the foot are particularly suitable and interesting for these analyses because static and dynamic alterations have large components in all three anatomical planes.

To date, 10 patients with severe adult flatfoot have been enrolled and treated with surgical correction of the deformity. They were examined with clinical and instrumental evaluation preoperatively and at 8 months postoperatively. They were imaged with WBCT while standing and a few minutes later with baropodometry[31,34] and full gait analysis using a eight-camera motion system (Vicon, Oxford, UK), and an established proprietary multisegment foot kinematic protocol[35,36] was performed. This protocol entails the acquisition of the 3D trajectory of three passive markers on the shank and the foot (►**Fig. 6**), the latter originally able to track in the 3D space absolute and relative motion of rear-, mid-, and forefoot segments assumed to be rigid, from which rotations at the ankle, Chopart, and Lisfranc joints are calculated. Because of its position and the relevant unavailability of palpable bony landmarks, the talus cannot be tracked separately in gait analysis, and motion of the overall ankle complex cannot be distinguished between that of the tibiotalar and subtalar joints. These 3D rotations are obtained together with the two major rotations of the first metatarsophalangeal joints, the angle of the medial longitudinal arch, and the inclination with respect to the ground of the first, second, and fifth metatarsal bones.[37]

The preoperative measurements established the severity of the flatfoot deformities in 3D and helped plan suitable corrections during surgery; postoperative measurements report the corresponding results obtained. Analyses of

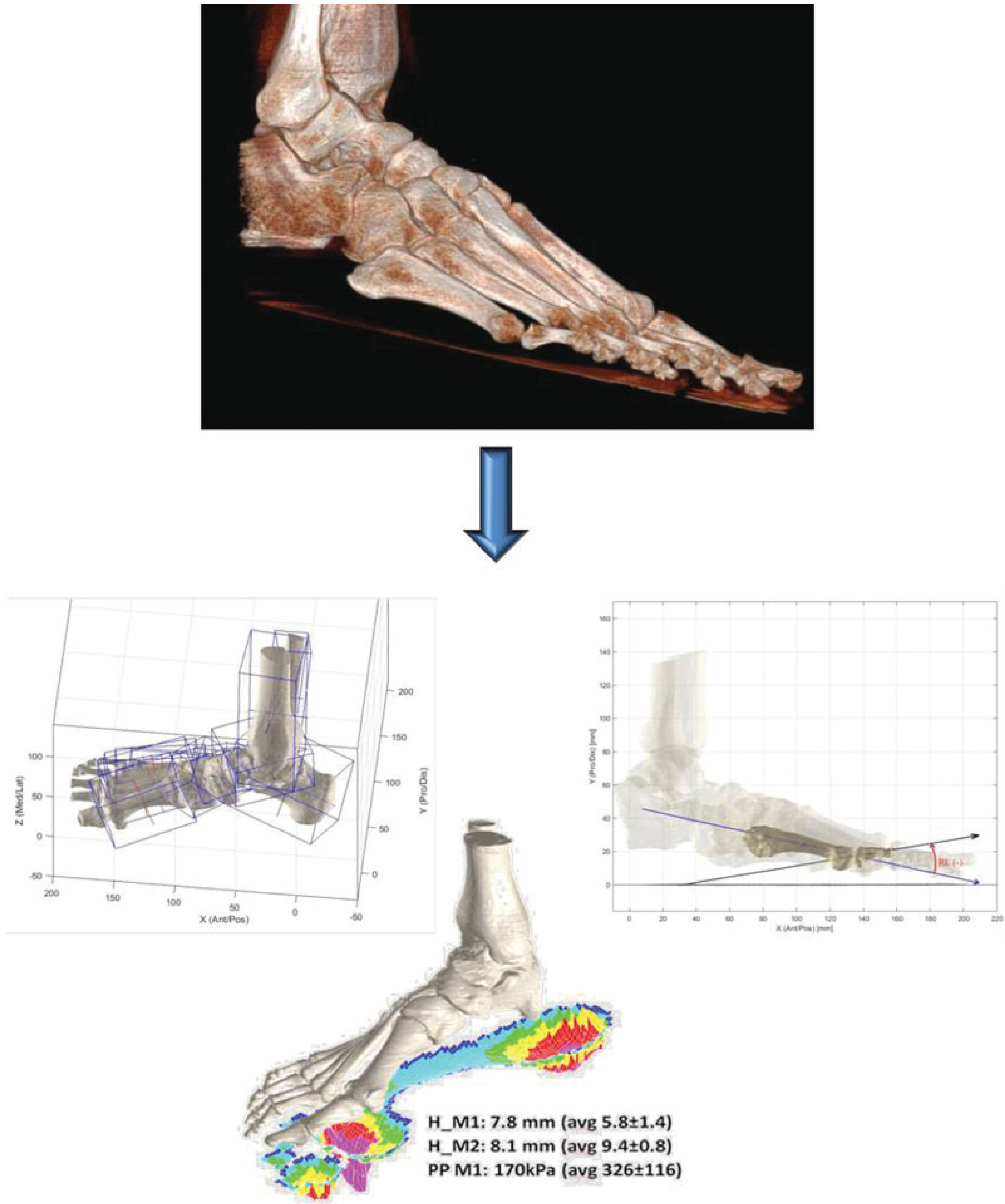

Fig. 5 Study of the diabetic foot. A three-dimensional (3D) rendering from the cone-beam computed tomography device (top), and images from the data analysis (bottom). Reference frames based on principal component analysis for all foot bones (left) in a single typical diabetic foot; calculation of the first metatarsophalangeal joint angle from relevant 3D bone models (right). The full foot model registered on the corresponding pressure footprint (bottom) from the same representative patient. Relevant values and averages of the main geometric parameters are depicted: the minimum height of the first (H_M1) and second (H_M2) metatarsal bones, and the peak pressure in the first metatarsal bone (PP M1) area of the footprint.

both will reveal anatomical and functional improvements after surgery. In particular, a reduction of dynamic hindfoot pronation is expected. The combination of the use of WBCT and gait analysis and relevant measurement correlations seems fundamental to finally provide accurate evaluations of flatfoot surgical corrections, in particular the assessment of subtalar joint alignment, that is, in pronation, standing, and walking conditions.

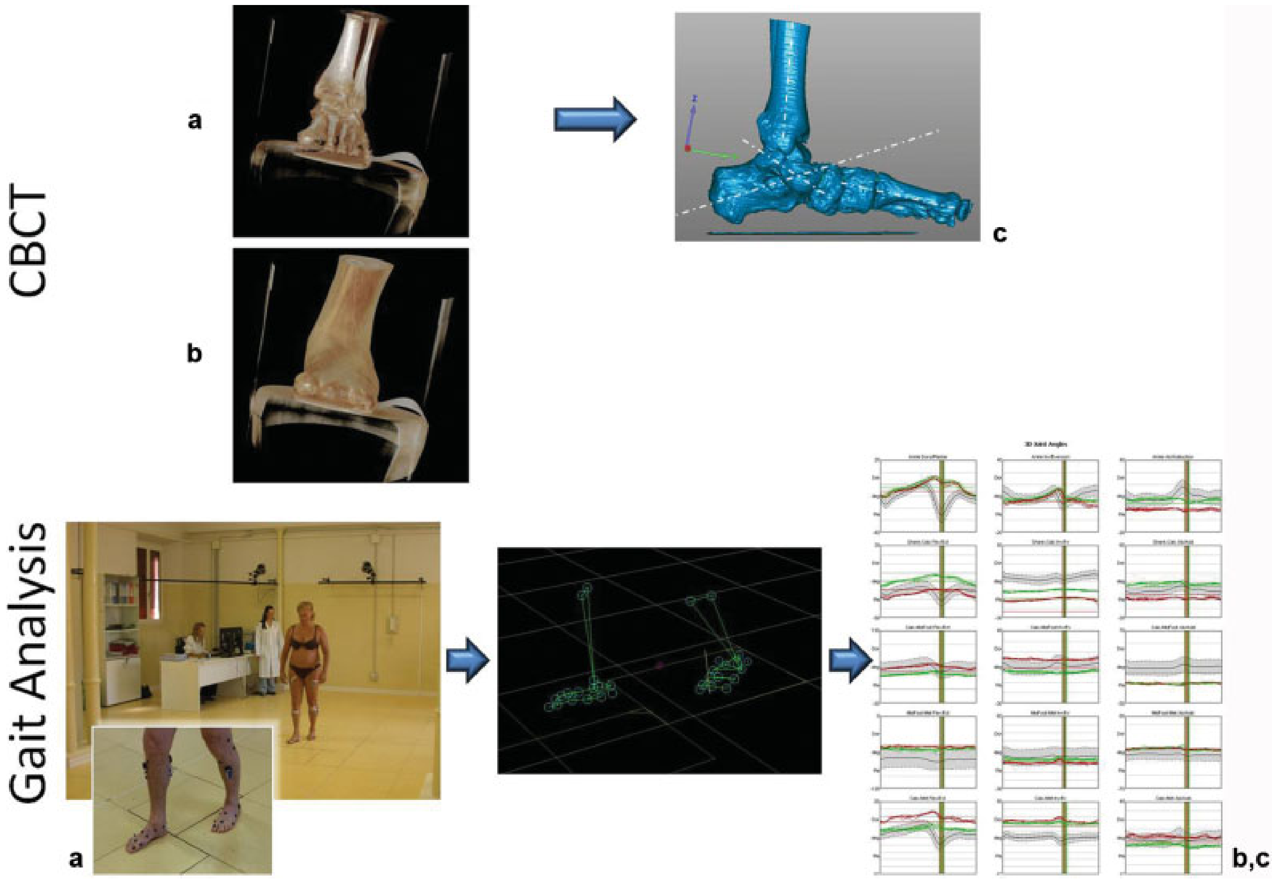

Fig. 6 Subtalar fusion study in cone-beam computed tomography (CBCT) first (top) and in the gait-analysis laboratory a few minutes later (bottom). In CBCT, different soft tissue filtering results in depicting the bones: (**a**) for following geometric analyses, by using a three-dimensional (3D) digital model of the foot bones (**c**). With these filters, even the skin can be depicted (**b**), and in case of segmented, for a possible final 3D reconstruction of the foot and ankle shape, for example for personalization of orthotics. In both, the cables for the concomitant plantar pressure data collection can be detected (out from the lateral side). In gait analysis, (**a**) optoelectronic cameras can track in the laboratory reference frame skin marker trajectories; the instrumented feet during this kinematics data collection are also depicted in the smaller frame. (**b**) Stick diagram of the markers in the double-support phase of walking. (**c**) The time history of the 3D rotations (columns) of the major foot joints (rows): the overall ankle joint: between the shank and the foot (top row), the ankle complex (second row), the Chopart (third), and Lisfranc (fourth) joints, and the overall motion between the forefoot and the rearfoot (bottom row).

Simultaneous Measurements

In several of these CBCT scan sessions, plantar pressure of the foot under load was collected simultaneously. Pressure at the interface between the bare foot and the step of the CBCT device was measured using the instrumented insoles of the Pedar system (Novel GmbH, Munich, Germany; pressure range: 15–600 kPa; nominal accuracy: 2.5–5 kPa). These have 99 sensors distributed all over the footprint, each sampling a value of pressure at a frequency of 50 Hz. Relevant instrumentation and overall encumbrance can be seen in ►**Figs. 4b**, **6a**, and **6b**.

From these continued measurements during the scan, the main standard pedobarographic parameters were calculated: the maximum force (% body weight), PP (kPa), and time-normalized PTI (kPa) (►**Fig. 7** shows the screenshot). These can be obtained separately for the rearfoot (0–30% insole length), midfoot (31–60% insole length), forefoot (61–100% insole length), and in the total foot.[38,39] PP is defined as the highest pressure recorded by any sensor in a region of interest; normalized PTI is defined as the integral of PP over the time of contact with the plantar region normalized to the stance duration. Analysis of these regional pedobarographic parameters is performed using ad hoc software written in MATLAB.

The value of these data are twofold. During the acquisition, the operators can check whether the required load is experienced exactly at the plantar aspect of the foot because these measurements can be controlled in real time; in addition, at the follow-up (i.e., after treatments, over a period of time, etc.), the same load distribution can be targeted exactly for a perfect replica of the same external conditions. In both cases, not only the overall parameters can be inspected, but also their distribution over the anatomical regions of the foot and progression over time during the execution of the radiographic scan. The observation from these preliminary results is that when full body weight is requested of the subject, only $\sim$ 90% is experienced.

Discussion

Quantification of 3D absolute and relative alignments of bone is now possible in upright single- or double-leg

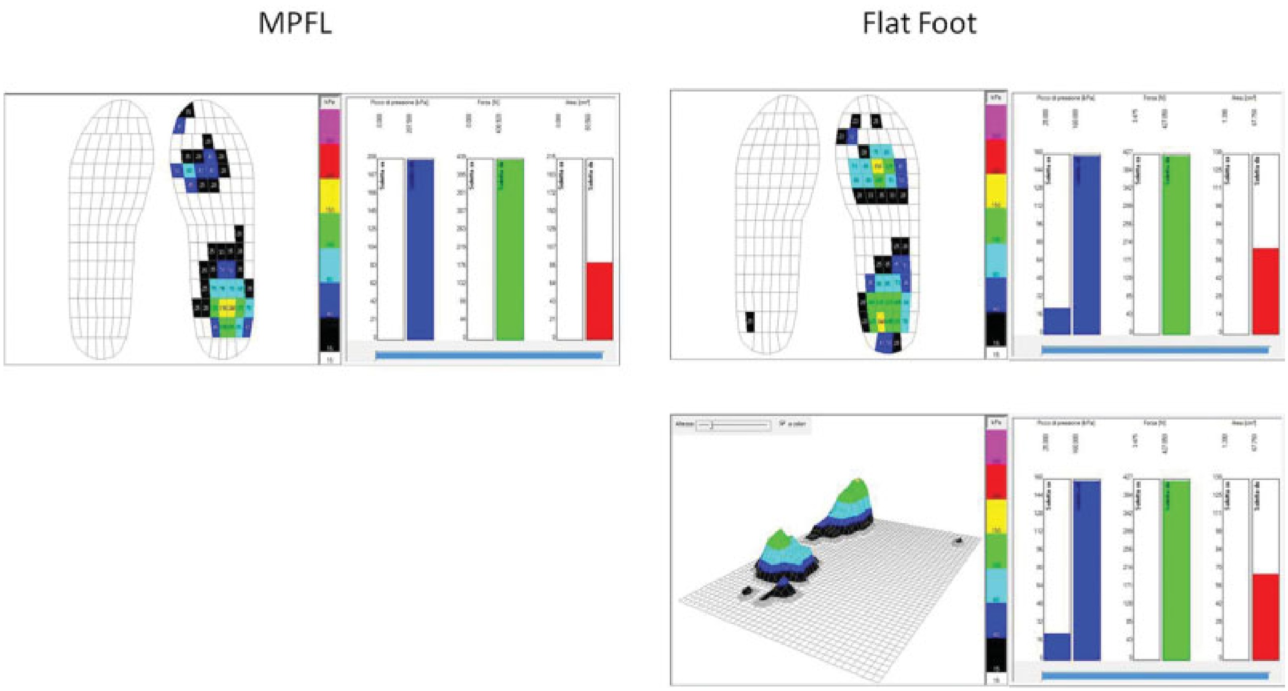

Fig. 7 Screenshots from typical plantar pressure measurements during scanning of a right foot, from the medial patellofemoral ligament (MPFL) (left) and the flat foot (right) studies. Two-dimensional graphical representation of the sensors over the footprint, each with the mean value of the pressure and a color map (left), and bar diagrams (right) with the main biomechanical parameters: peak pressure (blue), vertical force (green), and area (red). These values can also be represented for each sensor in three dimensions (below).

weight-bearing postures by several CBCT devices.[7] Previous measurements in weight-bearing were limited to 2D and affected by operator-dependent identification of alleged anatomical references. These devices also have the advantage of lower doses and imply a less restrictive regulation for radiation protection both for the operators and for the room environment; thus standard radiologic departments are no longer necessary for these. Another advantage is the original 3D volumetric format of the row data, from which traditional CT slices can be generated along any direction and with different resolutions. We discussed that the 3D view and weight-bearing conditions are both fundamental for the foot and ankle and for the knee joints, where the complexity of the pathologic conditions and treatment results can be revealed under realistic and subject-specific load. Hence the real status of bone and joint alignments can finally be assessed in 3D, both in terms of original deformities and after-treatment follow-up. Other encouraging evidence includes the shorter time spent by radiology technicians and therefore lower overall costs.

For decades, radiographic measurements of the foot and knee bones have been proposed, investigated, applied, and discussed.[11,16,40–42] These include single-bone absolute orientation, interbone relative alignments, distances, arch angles, and also morphological aspects of the single bones. A recent literature review[43] surveyed the most popular of these foot and ankle radiographic measures, although they are still based on weight-bearing radiographic images. That comprehensive review includes a careful aggregation of similar conceptual measures and relevant diagrammatic representations. The work was meant to be a baseline for future more comprehensive 3D definitions of bone alignments, taking advantage of the WBCT-based scans that overcome the limits of traditional CT and MRI (in 3D, but unloaded) and radiograph (under load, but in 2D) devices. A similar analysis[11] described traditional angular measures from radiographic images, although a large number of these are not applied, and a number are missing.

From these two comprehensive recent review articles, it is evident that existing foot and ankle angular measures also suffer from unclear or varying descriptions and calculation methods, thus resulting in inconsistent outcomes across studies. Moreover, no shared terminology has yet been established to describe absolute and relative bone orientations, and very similar measures are often reported with different names by different authors. For many of these measurements, a lack of consensus also exists for the radiographic view and the anatomical references. This could be partially explained by the interdisciplinary nature of this topic that involves radiologists, physicians, bioengineers, and technologists. This rather confusing scenario is possibly the cause for the large inter- and intraoperator variability of these measurements observed across studies in the literature.

The main limitations of traditional angular measurements, particularly those of foot and ankle bones, is that they are based on radiographic images. The orientation between radiographic beam and detector is operator dependent and therefore difficult to control across acquisitions over time. This affects how the anatomical part is projected on the radiograph, particularly in nonlateral views, where the beam inclination must also cope with the shank. Several possible radiographic views, and therefore of beam orientation, have been described:

lateral, anteroposterior of the foot or of the ankle: "mortise," hindfoot alignment or "Saltzman," and oblique. Also the beam focus has been set very differently: in the anteroposterior view of the foot, in the third cuneiform, at the base of the third metatarsal, or in the center of the navicular. All these inconsistencies result in large interobserver errors.[44–46]

Another important source of inaccuracy is the overall posture of the subject under analysis, and the exact positioning of the foot between the X-ray tube and the image plane.[47,48] Any metatarsal bone generates a different angle with respect to the ground when the bone is projected into the sagittal plane of the foot, even in cases in which the 3D inclination is the same. This was also discussed recently for multisegment in vivo kinematic analysis.[49,50] Among the challenges regarding control and repeatability of the data collection procedures with medical imaging instruments, the loading condition should be taught and monitored carefully, both in single- and double-leg upright postures; the full, half, and even null body weight, or any relevant modulation, may be acquired, obtained by simple ground reaction force devices. The overall skeletal structure of the foot is in fact influenced by the amount of load,[51,52] but ankle joint flexion, leg and foot axial rotation,[47,48] and even trunk inclination also have effects on this structure.

Some of the inconsistent results from the literature can be explained by possible variations in all these experimental conditions. This is particularly critical when preoperative versus postoperative assessments are obtained in the same patients. The foot and ankle positioning can be checked inductively, using for example the tibial inclination (the plantigrade angle),[11] although no adjustments are then possible. Finally, in addition to all these more experimental-related issues, there are also the subjective operator-dependent geometric analysis of the radiographs: the identification of anatomical landmarks, axes, or joint lines, still frequently performed with manual instruments. For these reasons, radiographic angles were shown to be not repeatable, resulting in unreliable clinical studies[53] known as "intrinsic imprecision."[54]

Some modern medical imaging devices now allow CT scans in weight-bearing,[6,7] finally giving access to thorough 3D geometric measurements of the foot and ankle bones under load. Because this condition was accessible for decades only for planar radiograph images,[11,55] novel 3D measures of the overall foot bone architecture now need to be defined carefully and established in the biomechanical and clinical communities. A recent study[56] analyzed and compared several original measurement techniques in a single real foot. The effects of malpositioning and deformity were also simulated by rotating the foot bone model about the vertical and anteroposterior axes. The measurement techniques affected the least were those in 3D and from PCA-based calculations. These are expected to be marginally affected by malpositioning and deformity because of their global and operator-independent calculations.

In these very recent articles and in the present initial applications in a clinical context, several possible innovative measures have been defined, starting from 3D models of the foot bones. Comparison with corresponding traditional 2D measures, that is, the radiographic angles, both as absolute and relative, will be necessary, however, to reveal possible differences, but the advantages and potential applications are many. The 3D view of the bones, in fact, in addition to the available digital format, allows more automatic calculations, reducing substantially the effect of manual identification of alleged references, such as bony landmarks and axes.[53,54] This seems particularly true for PCA-based calculations, which eliminate the tedious and critical manual identification of landmarks, but mainly they are very repeatable because they are automatic and not affected by foot malpositioning and deformity.[56] The 3D inclination with respect to the ground is also more consistent than any planar projection, as implied in any radiographic imaging of the bone.

In addition to the present 3D representations of traditional 2D radiographic angles, more advanced measures can also be established in the future including descriptive complex curves or even volumes, for example in the case of longitudinal or transverse arches of the foot. In addition to the techniques for bone axes definition reported here, that is, line segments through anatomical landmarks or middiaphyseal axes, many other options can be adopted by looking, for example, at different anatomical landmarks or projection techniques, or at different diaphyseal point cloud selections. The present report of preliminary studies is only an initial analysis of the mathematical and biomechanical tools to be potentially applied for the calculation of bone alignments. These can theoretically be applied in any 3D bone model of the foot or the knee, and also from standard CT and MRI, but of course they offer value mostly because of the weight-bearing condition.

Regarding weight-bearing, load can be modulated, including full single- or double-leg upright postures, or many other similar conditions such as half body weight, on tiptoe, or even with the ankle and the lower limb under known rotations.[32] Shoes and orthotics can also be scanned together with the anatomical structures. Synchronized measurements of plantar pressure may be collected by using standard devices such as instrumented platforms or insoles. These can be used for additional measurements but also to characterize carefully the exact loading conditions in each single scan.

WBCT still raises several issues and presents limitations. The effects of malposition of the overall foot, as well as of bone and joint deformities, will be investigated anyhow; a preliminary analysis revealed considerable effects for malposition and misalignment,[56] although this was based on computer simulations and applied on a single normal foot. It is expected, however, that foot deformities can aggravate the limitations of the measures based on 2D images. The ankle and knee joint position must be inspected carefully during data collection, along with the WBCT devices, and in all three anatomical planes, so as not to introduce associated variations to the relevant bone architecture. In general, the loading condition should be analyzed and defined very carefully. Double-leg posture does not guarantee equally distributed weight and may complicate 3D reconstructions; single-leg posture may not be consistent over time; full or partial leg bearing should be targeted according to the specific clinical interest; knee or ankle joint flexion, as well as axial rotation, should be carefully monitored.

Among the general issues for CBCT scans, there is also the limited field of measurement; in several of these devices, large-size feet cannot be scanned entirely. In that case, the area of major interest, for example the rearfoot or the forefoot, can be targeted, or both areas can be taken in two successive scans and then merged by shape matching or other spatial registration techniques,[30] with or without common technical or anatomical references. Computer-based 3D models of the bones are clearly necessary, and these can be obtained today only by time-consuming 3D reconstructions via segmentation of DICOM files; however, freeware software and robust modern tools can now facilitate this critical work.[57] If the immediate effect of shoes or orthotics is searched, some of the current techniques and algorithms may result in inaccurate bone alignments also in 3D and in weight-bearing, particularly when footwear alters largely the overall position of the foot bones, resulting in inconsistent comparisons. Finally, better filters for metal artifact are claimed, but these should be investigated carefully in specific, more technological studies.

For these devices in the future, overall ergonomic and loading conditions should be addressed and ameliorated, perhaps by using instruments for a quick prescan assessment of the exact posture and the real load. These can minimize intersession variability and therefore ensure preoperative-versus postoperative analyses; with suitable 3D registrations of the bone models, the comparison can be very precise.[58] Elementary maneuvers and simple clinical tests can be replicated within the bore, such as on tiptoe, Jack test, talar tilt, muscle strength exercise, and so on. It is expected that traditional 2D geometric measurements from radiographic images will be revisited, and new definitions of geometric measures will be proposed for thorough characterizations of the foot and knee joint physiology and pathology. In particular, thorough definitions of longitudinal axes of the bones, anatomical reference frames, and several other relevant descriptions will be defined. It might eventually be the case that direct measurements on the original 3D volume of the voxel will be possible, before any time-consuming 3D bone reconstruction. As discussed, radiation doses and generation of equivalent 3D bone models from the collected DICOM files are currently among the major barriers for the full exploitation of these 3D measures; however, these doses, and relevant image quality, as well as the virtual slicing, can both be modulated to adjust to the purpose. That is, the resolution sought for the individual clinical interest may be minimized when the technical specifications are not too demanding.

The present series of studies were presented from the perspective of an orthopaedic center, where bones and joints are clearly the major interest; nevertheless, the quality of these scans and the following 3D reconstructions, together with modern tools for relevant image segmentation, can also allow effective analyses of soft tissues. This can also be achieved by combining CBCT and MRI scans, as already shown for the ankle joint[30] a decade ago, and also for the temporomandibular joint complex.[59] Many additional applications are also expected in the area of assessment of shoes, orthotics, and insoles. Where this treatment is particularly critical (e.g., in orthopaedics or shoes for patients with diabetes), 3D scans with and without the footwear are of value, and they may reveal very carefully the true differing conditions of the internal structures. Certainly control populations will be necessary for most of these future studies, which would be demanding for the ethical aspects involved. Paradoxically, the overall bone architecture of a normal foot in weight-bearing in 3D is still not established. For all this, a new cultural education will be necessary for 3D knowledge of bone and joints of the lower limb. Improvement of cartilage imaging is expected to be achieved. Integration with kinematics, dynamics, and electromyographic measures will be developed.

With this review, full 3D geometric characterization of ankle, foot and knee bones architecture was also shown to be feasible in weight-bearing. We have focused on a single WBCT device, but concepts and procedures discussed here can easily be extended to others. In summary, both single-bone inclination, with respect to the ground, and relative joint angles, as routinely measured for decades on traditional radiographs, can now be obtained in 3D, with lower radiation doses, more consistency, and less operator dependence. The relevant 3D bone models can support more realistic preoperative planning and postoperative assessment; for the former, in case of severe damage of the bone or joint to be treated, the contralateral can be taken as the target.[60,61] This was initially demonstrated here for a few studies on the foot and knee, but extension to many other anatomical structures seems straightforward. It was also preliminary that the PCA technique, which automatically and therefore with full repeatability, detects an orthogonal coordinate system according to the three anatomical axes, can be used successfully to define operator-independent anatomical reference frames in 3D. With this technique, the effects of foot malpositioning and deformities were shown to be less critical. Other original measurements are expected to be developed, as already shown in a preliminary way.[62,63] Integration of these novel 3D measures of bone morphology with current kinematics or baropodometric analyses definitely has great potential, particularly for their synergy, and they will contribute to shed more light on the biomechanical status of these anatomical areas.

Funding Source
Ministero della Salute: http://dx.doi.org/10.13039/501100003196, Programma 5*1000.

Conflict of Interest
None declared.

References

1 Verhelst P, Verstraete L, Shaheen E, et al. Three-dimensional cone beam computed tomography analysis protocols for condylar remodelling following orthognathic surgery: a systematic review. Int J Oral Maxillofac Surg 2019; June 17 (Epub ahead of print)

2 Aydin U, Gormez O, Yildirim D. Cone-beam computed tomography imaging of dentoalveolar and mandibular fractures. Oral Radiol 2019; May 17 (Epub ahead of print)

3 Swennen GR, Schutyser F. Three-dimensional cephalometry: spiral multi-slice vs cone-beam computed tomography. Am J Orthod Dentofacial Orthop 2006;130(03):410–416

4 Ricci PM, Boldini M, Bonfante E, et al. Cone-beam computed tomography compared to X-ray in diagnosis of extremities bone fractures: a study of 198 cases. Eur J Radiol Open 2019; 6:119–121

5 Ludlow J, Ivanovic M. Weightbearing CBCT, MDCT, and 2D imaging dosimetry of the foot and ankle. Int J Diagnostic Imaging 2014; 1(02):

6 Ludlow JB. Hand-wrist, knee, and foot-ankle dosimetry and image quality measurements of a novel extremity imaging unit providing CBCT and 2D imaging options. Med Phys 2018;45(11): 4955–4963

7 Barg A, Bailey T, Richter M, et al. Weightbearing computed tomography of the foot and ankle: emerging technology topical review. Foot Ankle Int 2018;39(03):376–386

8 Lintz F, de Cesar Netto C, Barg A, Burssens A, Richter M; Weight Bearing CT International Study Group. Weight-bearing cone beam CT scans in the foot and ankle. EFORT Open Rev 2018;3(05): 278–286

9 Posadzy M, Desimpel J, Vanhoenacker F. Cone beam CT of the musculoskeletal system: clinical applications. Insights Imaging 2018;9(01):35–45

10 Hamard M, Neroladaki A, Bagetakos I, Dubois-Ferrière V, Montet X, Boudabbous S. Accuracy of cone-beam computed tomography for syndesmosis injury diagnosis compared to conventional computed tomography. Foot Ankle Surg 2019; April 1 (Epub ahead of print)

11 Lamm BM, Stasko PA, Gesheff MG, Bhave A. normal foot and ankle radiographic angles, measurements, and reference points. J Foot Ankle Surg 2016;55(05):991–998

12 Parr WC, Chatterjee HJ, Soligo C. Calculating the axes of rotation for the subtalar and talocrural joints using 3D bone reconstructions. J Biomech 2012;45(06):1103–1107

13 Kai S, Sato T, Koga Y, et al. Automatic construction of an anatomical coordinate system for three-dimensional bone models of the lower extremities—pelvis, femur, and tibia. J Biomech 2014;47 (05):1229–1233

14 Renault J-B, Aüllo-Rasser G, Donnez M, Parratte S, Chabrand P. Articular-surface-based automatic anatomical coordinate systems for the knee bones. J Biomech 2018;80:171–178

15 Saltzman CL, Nawoczenski DA, Talbot KD. Measurement of the medial longitudinal arch. Arch Phys Med Rehabil 1995;76(01): 45–49

16 Thomas JL, Kunkel MW, Lopez R, Sparks D. Radiographic values of the adult foot in a standardized population. J Foot Ankle Surg 2006;45(01):3–12

17 Rungprai C, Goetz JE, Arunakul M, et al. Validation and reproducibility of a biplanar imaging system versus conventional radiography of foot and ankle radiographic parameters. Foot Ankle Int 2014;35(11):1166–1175

18 Maynou C, Szymanski C, Thiounn A. The adult cavus foot. EFORT Open Rev 2017;2(05):221–229

19 Menz HB, Munteanu SE, Zammit GV, Landorf KB. Foot structure and function in older people with radiographic osteoarthritis of the medial midfoot. Osteoarthritis Cartilage 2010;18(03):317–322

20 Gwani AS, Asari MA, Mohd Ismail ZI. How the three arches of the foot intercorrelate. Folia Morphol (Warsz) 2017;76(04):682–688

21 Zhou Y, Zhou B, Liu J, et al. A prospective study of midfoot osteotomy combined with adjacent joint sparing internal fixation in treatment of rigid pes cavus deformity. J Orthop Surg Res 2014;9:44

22 Giannini S, Leardini A, O'Connor J. Total ankle replacement: review of the designs and of the current status. Foot Ankle Surg 2000;6(02):77–88

23 Leardini A, O'Connor JJ, Catani F, Giannini S. Mobility of the human ankle and the design of total ankle replacement. Clin Orthop Relat Res 2004;(424):39–46

24 Leardini A, O'Connor JJ, Giannini S. Biomechanics of the natural, arthritic, and replaced human ankle joint. J Foot Ankle Res 2014;7 (01):8

25 Omar IM, Abboud SF, Youngner JM. Imaging of total ankle arthroplasty: normal imaging findings and hardware complications. Sem Musculoskelet Radiol 2019;23(02):177–194

26 Liverani E, Fortunato A, Leardini A, et al. Fabrication of Co–Cr–Mo endoprosthetic ankle devices by means of Selective Laser Melting (SLM). Materials Design 2016;106:60–68

27 Wang X, Xu S, Zhou S, et al. Topological design and additive manufacturing of porous metals for bone scaffolds and orthopaedic implants: a review. Biomaterials 2016;83:127–141

28 Belvedere C, Siegler S, Fortunato A, et al. New comprehensive procedure for custom-made total ankle replacements: medical imaging, joint modeling, prosthesis design, and 3D printing. J Orthop Res 2019;37(03):760–768

29 Giannini S, Romagnoli M, O'Connor JJ, Malerba F, Leardini A. Total ankle replacement compatible with ligament function produces mobility, good clinical scores, and low complication rates: an early clinical assessment. Clin Orthop Relat Res 2010;468(10):2746–2753

30 Durastanti G, Leardini A, Siegler S, Durante S, Bazzocchi A, Belvedere C. Comparison of ankle articular surfaces among morphological models derived from different medical imaging technologies. Quant Imaging Med Surg. In press

31 Giacomozzi C, Leardini A, Caravaggi P. Correlates between kinematics and baropodometric measurements for an integrated in-vivo assessment of the segmental foot function in gait. J Biomech 2014;47(11):2654–2659

32 Hirschmann A, Pfirrmann CW, Klammer G, Espinosa N, Buck FM. Upright cone CT of the hindfoot: comparison of the non-weight-bearing with the upright weight-bearing position. Eur Radiol 2014;24(03):553–558

33 Giacomozzi C, Martelli F, Nagel A, Schmiegel A, Rosenbaum D. Cluster analysis to classify gait alterations in rheumatoid arthritis using peak pressure curves. Gait Posture 2009;29(02):220–224

34 Caravaggi P, Leardini A, Giacomozzi C. Multiple linear regression approach for the analysis of the relationships between joints mobility and regional pressure-based parameters in the normal-arched foot. J Biomech 2016;49(14):3485–3491

35 Leardini A, Benedetti MG, Berti L, Bettinelli D, Nativo R, Giannini S. Rear-foot, mid-foot and fore-foot motion during the stance phase of gait. Gait Posture 2007;25(03):453–462

36 Portinaro N, Leardini A, Panou A, Monzani V, Caravaggi P. Modifying the Rizzoli foot model to improve the diagnosis of pes-planus: application to kinematics of feet in teenagers. J Foot Ankle Res 2014;7(01):754

37 Caravaggi P, Lullini G, Berti L, Giannini S, Leardini A. Functional evaluation of bilateral subtalar arthroereisis for the correction of flexible flatfoot in children: 1-year follow-up. Gait Posture 2018; 64:152–158

38 Caravaggi P, Giangrande A, Berti L, Lullini G, Leardini A. Pedobarographic and kinematic analysis in the functional evaluation of two post-operative forefoot offloading shoes. J Foot Ankle Res 2015;8 (01):59

39 Caravaggi P, Giangrande A, Lullini G, Padula G, Berti L, Leardini A. In shoe pressure measurements during different motor tasks while wearing safety shoes: the effect of custom made insoles vs. prefabricated and off-the-shelf. Gait Posture 2016;50:232–238

40 Steel MW III, Johnson KA, DeWitz MA, Ilstrup DM. Radiographic measurements of the normal adult foot. Foot Ankle 1980;1(03): 151–158

41 Gentili A, Masih S, Yao L, Seeger LL. Pictorial review: foot axes and angles. Br J Radiol 1996;69(826):968–974

42 Marzo J, Kluczynski M, Notino A, Bisson L. Comparison of a novel weightbearing cone beam computed tomography scanner versus a conventional computed tomography scanner for measuring patellar instability. Orthop J Sports Med 2016;4(12):2325967116673560

43 Carrara C, Caravaggi P, Belvedere C, Leardini A. Radiographic angular measurements of the foot and ankle in weight-bearing: a literature review. Foot Ankle Surg 2019; July 31 (Epub ahead of print)
44 Gonzalez TA, Ehrlichman LK, Macaulay AA, et al. Determining measurement error for Bohler's angle and the effect of X-ray obliquity on accuracy. Foot Ankle Spec 2016;9(05):409–416
45 Neri T, Barthelemy R, Tourné Y. Radiologic analysis of hindfoot alignment: comparison of Méary, long axial, and hindfoot alignment views. Orthop Traumatol Surg Res 2017;103(08):1211–1216
46 Barg A, Harris MD, Henninger HB, et al. Medial distal tibial angle: comparison between weightbearing mortise view and hindfoot alignment view. Foot Ankle Int 2012;33(08):655–661
47 Dayton P, Feilmeier M, Hirschi J, Kauwe M, Kauwe JS. Observed changes in radiographic measurements of the first ray after frontal plane rotation of the first metatarsal in a cadaveric foot model. J Foot Ankle Surg 2014;53(03):274–278
48 Buck FM, Hoffmann A, Mamisch-Saupe N, Espinosa N, Resnick D, Hodler J. Hindfoot alignment measurements: rotation-stability of measurement techniques on hindfoot alignment view and long axial view radiographs. AJR Am J Roentgenol 2011;197(03):578–582
49 Leardini A, Caravaggi P, Theologis T, Stebbins J. Multi-segment foot models and their use in clinical populations. Gait Posture 2019;69:50–59
50 Caravaggi P, Matias AB, Taddei UT, Ortolani M, Leardini A, Sacco ICN. Reliability of medial-longitudinal-arch measures for skin-markers based kinematic analysis. J Biomech 2019;88:180–185
51 Shereff MJ, DiGiovanni L, Bejjani FJ, Hersh A, Kummer FJ. A comparison of nonweight-bearing and weight-bearing radiographs of the foot. Foot Ankle 1990;10(06):306–311
52 Shelton T, Singh S, Kreulen C, Giza E. The influence of percentile weight bearing on foot radiographs. Foot Ankle Spec 2018; October 21 (Epub ahead of print)
53 Guo C, Zhu Y, Hu M, Deng L, Xu X. Reliability of measurements on lateral ankle radiographs. BMC Musculoskelet Disord 2016;17(01):297
54 Saltzman CL, Brandser EA, Berbaum KS, et al. Reliability of standard foot radiographic measurements. Foot Ankle Int 1994; 15(12):661–665
55 Lin CS, Wu TY, Wang TM, Hou SM, Shih KS, Liaw CK. A new technique to increase reliability in measuring the axis of bone. J Foot Ankle Surg 2016;55(01):106–111
56 Carrara C. 3D measurements of foot bone architecture in weight-bearing by cone-beam computed tomography. Paper presented at: Congress XXVII of the International Society of Biomechanics; July 31, 2019; Calgary, Canada
57 Matsiushevich K, Belvedere C, Leardini A, Durante S. Quantitative comparison of freeware software for bone mesh from DICOM files. J Biomech 2019;84:247–251
58 Peiffer M, Belvedere C, Clockaerts S, et al; WBCT ISG. Three-dimensional displacement after a medializing calcaneal osteotomy in relation to the osteotomy angle and hindfoot alignment. Foot Ankle Surg 2018; December 7 (Epub ahead of print)
59 Hussain AM, Packota G, Major PW, Flores-Mir C. Role of different imaging modalities in assessment of temporomandibular joint erosions and osteophytes: a systematic review. Dentomaxillofac Radiol 2008;37(02):63–71
60 Belvedere C, Cadossi M, Mazzotti A, Giannini S, Leardini A. Fluoroscopic and gait analyses for the functional performance of a custom-made total talonavicular replacement. J Foot Ankle Surg 2017;56(04):836–844
61 Giannini S, Cadossi M, Mazzotti A, Ramponi L, Belvedere C, Leardini A. Custom-made total talonavicular replacement in a professional rock climber. J Foot Ankle Surg 2016;55(06):1271–1275
62 Lintz F, Welck M, Bernasconi A, et al. 3D biometrics for hindfoot alignment using weightbearing CT. Foot Ankle Int 2017;38(06): 684–689
63 Zhang JZ, Lintz F, Bernasconi A, Zhang S, Zhang S; Weight Bearing CT International Study Group. 3D biometrics for hindfoot alignment using weightbearing computed tomography. Foot Ankle Int 2019;40(06):720–726